

Membrane-sealed hollow microneedles and related administration schemes for transdermal drug delivery

Niclas Roxhed · Patrick Griss · Göran Stemme

Published online: 17 October 2007
© Springer Science + Business Media, LLC 2007

Abstract This paper presents fabrication and testing of membrane-sealed hollow microneedles. This novel concept offers the possibility of a sealed microneedle-based transdermal drug delivery system in which the drug is stored and protected from the environment. Sealed microneedles were fabricated by covering the tip openings of out-of-plane silicon microneedles with thin gold membranes. In this way a leak-tight seal was established which hinders both contamination and evaporation. To allow drug release from the microneedles, three different methods of opening the seals were investigated: burst opening by means of pressure; opening by applying a small voltage in the presence of physiological saline; and opening as a result of microneedle insertion into the skin. It was found that a 170 nm thick gold membrane can withstand a pressure of approximately 120 kPa. At higher pressures the membranes burst and the microneedles are opened up. The membranes can also be electrochemically dissolved within 2 min in saline conditions similar to interstitial fluid present in the skin. Moreover, through *in vivo* tests, it was demonstrated that 170 nm thick membranes break when the microneedles were inserted into skin tissue. The proposed concept was demonstrated as a feasible option for sealing hollow microneedles. This enables the realization of a closed-package transdermal drug delivery system based on microneedles.

Keywords Transdermal drug delivery · Intradermal drug delivery · Microneedles · Membrane · MEMS

1 Introduction

Patch-based transdermal drug delivery offers a convenient way to administer drugs without the drawbacks of standard hypodermic injections such as in patient acceptability and injection safety (Levine 2003). However, a major disadvantage of patch-based transdermal delivery is that it is limited to pharmaceutical substances that can diffuse through the skin barrier. In recent years, attention has been drawn to a new way of deliver macromolecular substances by using miniaturized needles to penetrate the skin barrier (Prausnitz 2004). These, so-called, microneedles would only penetrate the outermost skin layers, superficial enough to not reach receptors in the lower nerve-rich regions of the dermis. As a consequence, the stimulus caused by microneedle insertion into skin is weak and perceived as painless (Kaushik et al. 2001; Sivamani et al. 2005).

Until now, most of the research have been focused on microneedle fabrication and, to some extent, pre-clinical testing of microneedle-aided drug delivery. A large variety of microneedle designs have been proposed, including both hollow (McAllister et al. 2003; Gardeniers et al. 2003; Griss and Stemme 2003; Teo et al. 2005; Stoeber and Liepmann 2005) and non-hollow (Henry et al. 1998; Lin et al. 2001; Matriano et al. 2002; Mikszta et al. 2002; Martanto et al. 2004; Park et al. 2005) needles made from various materials. For drug delivery, non-hollow needles are limited to delivery schemes where the needles are either pre-coated

N. Roxhed (✉) · P. Griss · G. Stemme
Microsystem Technology Laboratory,
School of Electrical Engineering,
KTH—Royal Institute of Technology,
SE-100 44 Stockholm, Sweden
e-mail: niclas.roxhed@ee.kth.se

with the drug or only used to create perforations in the skin for subsequent topical drug administration. As a consequence, only a small amount of drug can be delivered by this method. In general however, non-hollow needles are easier to fabricate and are easier to make sharp. Sharp microneedles, in turn, are essential to ensure reliable skin penetration as the insertion force has been found to depend approximately linearly on the needle tip area (Davis et al. 2004). Hollow microneedles on the other hand, permit continuous infusion into the skin and allow for larger amounts to be delivered. To ensure good penetration properties also with hollow needles, our group introduced side-opened microneedles where the needle bore-opening is located on the side of the needle so that the needle still can have a sharp and well defined tip (Griss and Stemme 2003; Roxhed et al. 2007a).

Although, microneedles have shown to be a feasible method to deliver drugs into the tissue, many issues are yet to be investigated. More specific, issues concerning reliability in both skin penetration and liquid infusion need more attention as well as packaging concerns of microneedle-based system. This paper addresses the latter in which out-of-plane silicon microneedles are sealed with a thin membrane to provide a closed-package system. This novel concept was tested and schemes on opening the seals at the time of delivery were investigated.

2 Sealed hollow microneedles

2.1 Benefits of sealed microneedles

To achieve increased liquid absorption, microneedles are mostly arranged into two-dimensional arrays allowing delivery and liquid uptake over a larger area of the skin. Being inherently short, microneedles are also well suited to be integrated with a patch-like structure containing a drug reservoir and some kind of mechanism that drives the drug through the needles and into the skin (e.g. a pump or dispenser). In this way, a drug delivery system is achieved having essentially the same favorable properties as a conventional passive transdermal patch (e.g. nicotine patch), such as ease-of-use, unobtrusiveness and painlessness. Such a microneedle-based patch containing a compact, thermally actuated, liquid dispenser was introduced by us in earlier work (Roxhed et al. 2007b). Figure 1 shows a conceptual drawing of such a microneedle-based patch system.

Given a system like the one outlined in Fig. 1; the drug stored in the patch is exposed to the ambient

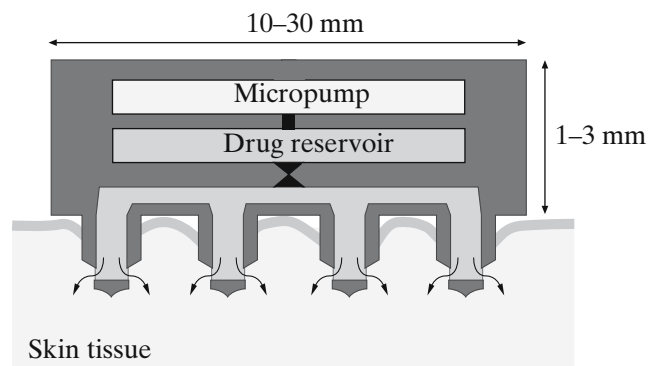


Fig. 1 Conceptual drawing of a microneedle-based drug delivery system

air through the hollow needles. To protect the drug from degradation, evaporation and leaking out from the patch, a suitable way is to seal the needle openings with thin leak-tight membranes. By this, the drug is well confined to the patch and can be stored for longer times, thus improving shelf-life.

Besides storage reasons, membrane seals can withstand pressure allowing both the drug to be packaged under pressure and providing a protection against, unintended, external pressure during device handling. In addition, sealed microneedles provide means for sophisticated delivery schemes and ways to avoid leakage caused by the irregularities of the skin. Since microneedles of a few hundred micrometers can be in the same length as recess structures in the skin, e.g. hair follicles, glands or wrinkles, local leakage might occur during liquid injection. This situation is illustrated in Fig. 2. By only open needle membranes that are in the dermal tissue, local leakage as described above can be avoided.

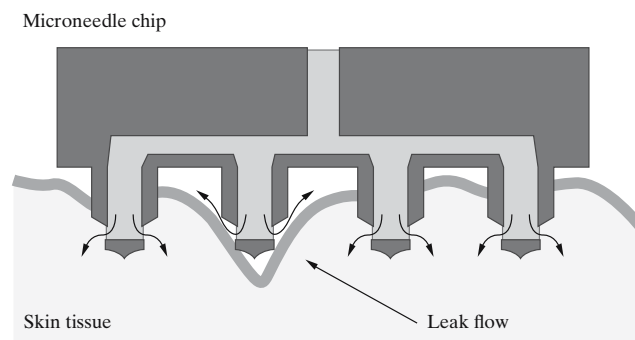


Fig. 2 Illustration showing penetration of microneedles into the skin tissue. Inhomogeneities in the tissue could be in the same order as the length of the needles resulting in a leakage flow

2.2 Opening schemes

Naturally, sealed microneedles need to be opened at the time of the delivery. A straightforward approach is to burst the seal by means of pressure generated by the dispensing mechanism. This however, does not exclusively open needles that penetrated the tissue.

A better approach is to break the seal when penetration occurs. With an appropriate geometrical configuration, thin membrane seals can be designed to break as a result of the forces involved when the needle penetrates the skin tissue. Providing even more opportunities to selectively control opening of the seal, the membrane can be dissolved once inserted into the tissue and in contact with interstitial fluid present under the skin barrier. A similar approach was introduced by Santini et al. for controlled drug release from implantable silicon microchips (Santini et al. 2000). In these devices, gold membranes covering drug reservoirs were dissolved through stimulated galvanic corrosion. I.e. an electrical potential was applied to the membrane and in the presence of an electrolyte (physiological saline), the gold layer was electrochemically etched and disrupted within a few seconds.

Since only membranes in contact with saline-containing interstitial fluid can be dissolved, the same method may be employed to selectively open microneedles that penetrated and are in the dermal tissue. Like the system presented in (Santini et al. 2000), the method also provides means of controlled release through individual microneedles, enabling drug release at specific times. The opening procedures described above are illustrated in Fig. 3.

A drawback of all of these methods is that residues from the membranes might detach from the needle and remain in the skin tissue after the patch has been used and removed. Hence, biocompatibility of the membrane material is essential in order to not introduce any

local inflammations. From that perspective biodegradable materials such as PLA (polylactide acid) or PLGA (polylactic-co-glycolic acid) would be preferred membrane materials. However, as for all polymers, they do not provide a hermetic seal and evaporation through the membrane will occur. On the other hand, the mass of a thin-film membrane (a few hundred nanometers thick) covering a relatively small microneedle opening (say $2,000 \mu\text{m}^2$), is a few nanograms. For a microneedle array with hundreds of needles, the total mass would be a few micrograms. Thus, because of the minute mass, choosing a bioinert membrane material, either a metal or a ceramic, might be a sufficient measure to ensure biocompatibility while still accomplishing a hermetic seal.

Nevertheless, as biocompatibility always needs to be assessed for a specific application (i.e. microneedle residues in the epidermal/dermal space at a specific body location) and duration (in relation to epidermal turnover times and the frequency of usage); the issue of biocompatibility remains of great importance but can not be ruled out without a full empirical study for the current application. Therefore, the study was limited to minimizing the risk for toxicological reactions and a material was chosen that is proven to possess a low likelihood to generate a harmful host response.

In this work, gold was used as the membrane material to achieve sealed hollow microneedles. Gold was chosen based on its well-known biocompatible properties, ability to provide a hermetic seal and compatibility with microfabrication processes. The latter giving the possibility to control the membrane thickness and thus the mechanical strength. The needles were fabricated using microfabrication batch techniques and the different opening schemes were tested and evaluated.

3 Fabrication

Arrays of hollow microneedles were fabricated using deep reactive ion etching (DRIE) of monocrystalline silicon. The needles were etched from 600 μm thick, 100 mm, standard wafers using a two-mask process combining isotropic dry etching and anisotropic etching. Figure 4 shows the essential etching steps of the process. A more detailed description of the fabrication process of side-opened hollow microneedles can be found in (Griss and Stemme 2003; Roxhed et al. 2007a).

As can be seen in Fig. 4, the microneedles were made hollow by etching the needle so that the bore intersects with the outer needle profile. To prevent etching inside the bore, the bore was passivated with a thermally grown silicon dioxide layer. Hence, after

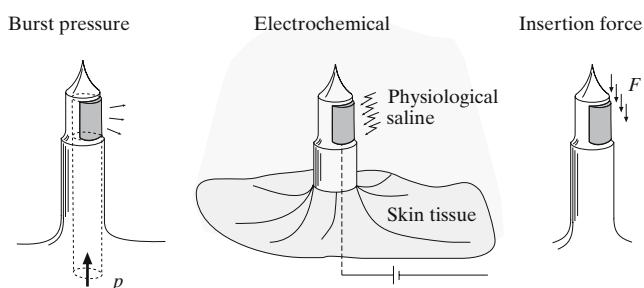


Fig. 3 Illustration of the three investigated opening schemes. From the left: opening by means of pressure, *in situ* electrochemically enhanced opening in the presence of saline and opening by the forces involved during needle insertion into the tissue (e.g. shear force)

the front side microneedle etch, the microneedle bore opening is covered by the oxide layer. This layer acts as structural support for the membranes sealing the microneedle openings.

Gold layers of three different thicknesses were evaporated onto the needles, 150, 300 and 450 nm thick. For all thicknesses, a 20 nm thick chromium adhesion layer was used. To ensure uniform coating, a 45° tilting and rotating mechanism was used to hold the wafer during the evaporation.

The oxide layer supporting the gold membranes was removed by means of HF vapor entering the needle bore from the backside. This was achieved by placing the microneedle wafer 1 cm above the liquid surface of 50% HF for 14 h.

Two different microneedle designs were fabricated and provided with sealing gold membranes: cross-shaped microneedles with the length of 310 μm and circular-shaped microneedles with the length of 400 μm . The latter having improved skin penetration properties, as described and evaluated in earlier work (Roxhed et al. 2007a). Figure 5 shows SEM pictures

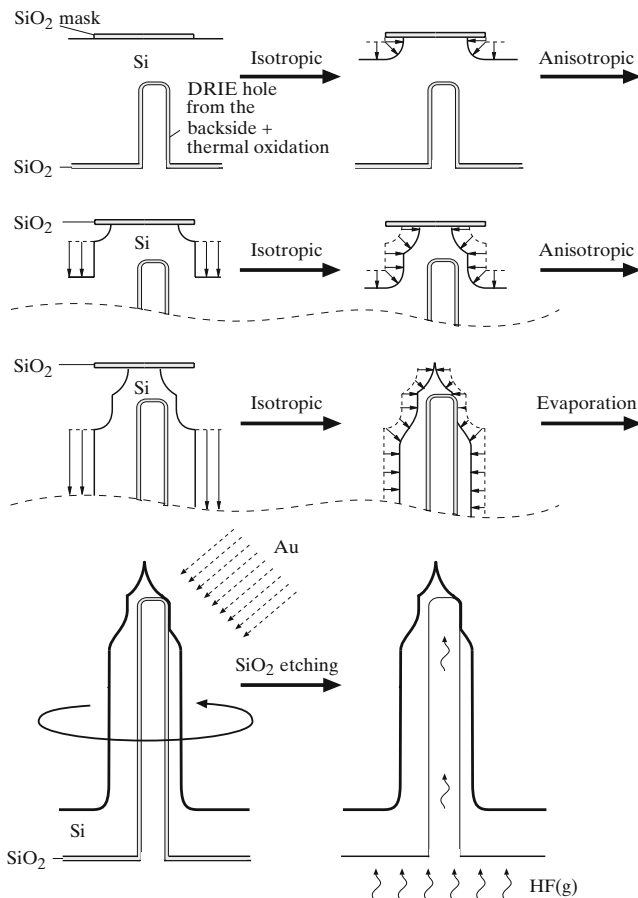


Fig. 4 Process flow of the fabrication of circular side-opened hollow microneedles

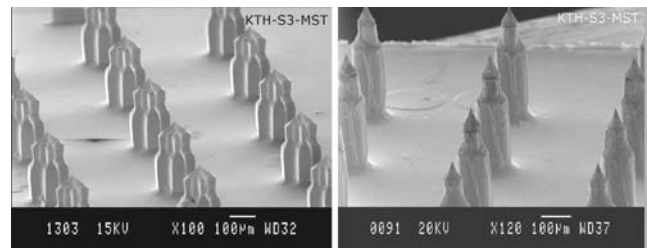


Fig. 5 Gold membrane sealed side-open hollow microneedles. (a) 310 μm long cross-shaped microneedles. (b) 400 μm long circular-shaped microneedles

of gold membrane sealed microneedles of both types. To obtain individual microneedle chips, the wafers were diced into $4 \times 4 \text{ mm}^2$ chips containing 25 needles pitched 500 μm apart.

4 Experimental

The seal of the microneedles was tested in different aspects. Tests on breaking the seals were performed for the three different opening schemes illustrated Fig. 3. Breaking by means of pressure and electrochemical enhanced corrosion were tested *in vitro*; seal breakage as a result of skin insertion was tested *in vivo*. The ability of the membrane to form a gas-tight seal was evaluated by measuring the liquid loss over time through sealed microneedles mounted on liquid reservoirs.

4.1 Opening by burst pressure

The pressure needed to burst the membranes of the microneedles was measured using a high-speed microscope camera (PixeLINK PL-A654) synchronized with a computer-based measurement system running Labview™ registering the applied pressure. The microneedle chip was pneumatically connected by pressing a slightly melted end of a short polyurethane tube to the backside of the chip. A pressure sensor (Motorola MPX2200DP) was inserted in connection to the polyurethane tube and electrically connected to the computer's data acquisition card. To achieve bursting, a pneumatic step signal with a rise time of approximately 15 s was applied to the back of the chip while microscope images of the microneedles were recorded. In order to clearly visualize the membrane burst, the microneedle chip was submerged in water just below the water surface and the occurrence of air bubbles was used to determine burst. Since the pressure signal and the recorded frames were synchronized, the burst pressure could be determined.

Three different membrane thicknesses (170, 320 and 470 nm) were tested using the cross-shaped microneedle design (Fig. 5(a)). Of the cross-shaped design, each microneedle features four membrane-covered, 2,080 μm^2 large, openings.

4.2 Electrochemical opening

Electrochemical opening of the gold film sealed microneedles was tested *in vitro*. The gold layer of the microneedle chip was contacted and used as the anode. A gold coated cathode was placed at a distance of 1 cm from the anode. Phosphate buffered saline (PBS, pH 7.4, 0.15 M NaCl) was used as electrolyte, resembling the properties of interstitial fluid (Fogh-Andersen et al. 1995). A voltage of +1.04 V relative to a saturated calomel reference electrode (SCE) was then applied to the sealing gold film. This particular voltage is used because the formation of water-soluble chlorogold(III) complexes is favored around this potential (Santini et al. 2000).

Also for this test, cross-shaped microneedles were used and the membrane thickness was 170 nm.

4.3 Opening through skin insertion

Breaking the seal of the microneedles by only inserting them into the skin was tested on human skin *in vivo*. Fifteen insertion tests were made using gold-membrane-sealed (170 nm thick) microneedle chips of the circular microneedle design (Fig. 5(b)). The circular microneedles were used since this particular design allows reliable skin penetration without the use of any special insertion tools or treatments. Ten of the 15 tests were made on an insertion site, approximately 3 cm proximal to the thumb knuckle, where the needles are known to reliably penetrate the tissue. The remaining five tests were made on an insertion site with very poor mechanical support where penetration is less reliable. For this, insertion was made on fatty tissue, 1–2 cm proximal to the medial part of the elbow bent at an angle of approximately 30°.

On both insertion sites, the needle chip was inserted by placing it onto the skin of the test subject (28-years-old, Caucasian male), and then applying a small force by hand. After the insertion, the needle chip was removed and inspected in an optical microscope where the number of broken membranes was counted. The test was performed in accordance with relevant regulations on human testing and informed consent was given.

4.4 Seal tightness evaporation test

The gold membranes of the sealed microneedle chip were tested as an evaporation barrier by comparing a sealed microneedle chip with an unsealed chip. The evaporation test was made at an elevated temperature where microneedle chips attached to a liquid reservoir were stored at 50°C and a relative humidity between 8 and 10% for 6 days. Cross-shaped microneedle chips were glued to DI-water filled glass capillaries and the liquid evaporation was measured by recording the location of the liquid meniscus with a digital camera every 15 min. Microneedle chips, containing 25 needles, have a total needle opening area corresponding to 0.052 mm^2 . For the sealed microneedle chip, membranes with the thickness of 170 nm was used. The chips were glued to the open end of the capillary using low viscosity cyanoacrylate and a thick layer of epoxy to minimize the leak from the bond interface.

5 Results

Figure 6 shows a bar plot of the measured pressure needed to break the seal of the microneedles. Three tests were made for each membrane thickness. The thinnest membrane, 170 nm thick, can withstand an over pressure as high as 120 kPa before bursting, thicker membranes were measured to burst at higher pressures. Although the number of trials are small, the

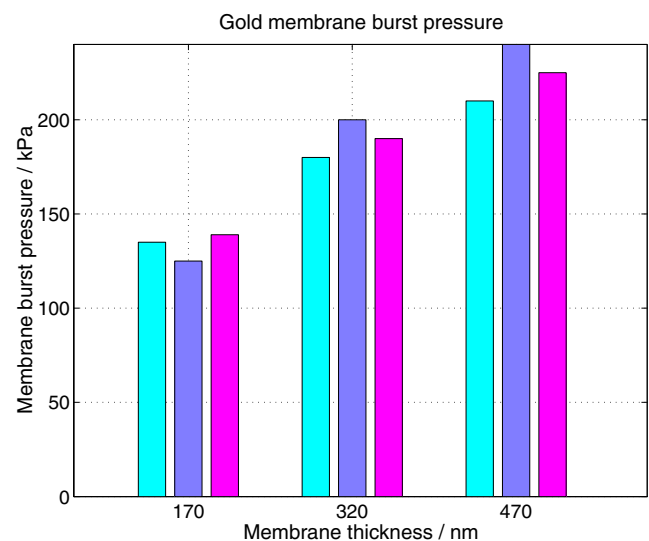
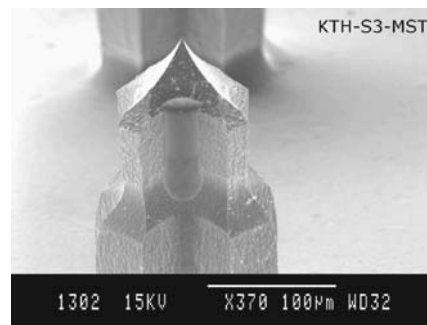
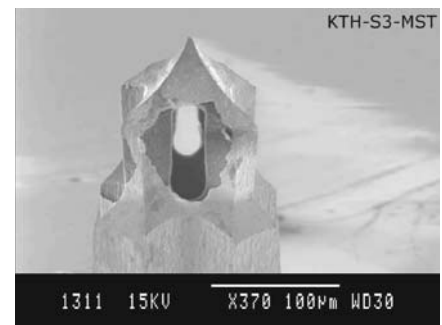


Fig. 6 Measurements showing the pressure needed to burst open the sealing gold membranes on the microneedles for different membrane thicknesses. Three burst tests are made for each thickness. For the membrane thickness of 470 nm one test chip did not burst at the maximum pressure load of 240 kPa

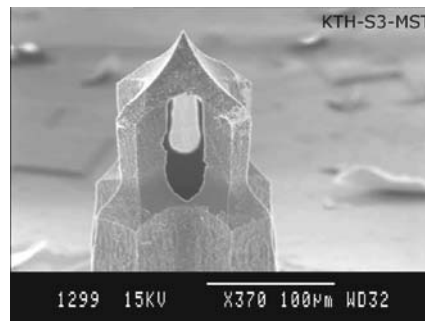
Fig. 7 SEM pictures of the tip part of the cross-shaped microneedle before and after removal of the sealing gold membranes



(a) Microneedle gold membrane before removal. The dimension of the membrane is $30\ \mu\text{m}$ by $70\ \mu\text{m}$.



(b) Microneedle gold membrane removed by means of air pressure.



(c) Microneedle gold membrane removed in vitro by means of an electrochemical reaction dissolving the gold layer within 2 min.

deviation between the three needle chips for a given membrane thickness is relatively low. Figure 7 shows close-up SEM pictures of a microneedle membrane before (Fig. 7(a)) and after (Fig. 7(b)) burst.

Tests on electrochemically breaking the microneedle seal showed that the $170\ \text{nm}$ thick gold membrane was fully etched within 2 min and the needle was thus opened up. Figure 7(c) shows a SEM picture of a needle opening after applying the electrochemical opening procedure. As the electrochemical reaction is diffusion limited, the time to dissolve the membrane is proportional to the thickness. Hence, a thinner membrane would need less time to be removed.

Insertion of the sealed microneedles into the skin showed that the membrane breaks by pure insertion. In total, 15 microneedle chips were tested and inspected, each having 25 needles. From the ten tests made on an insertion site were the needles are known to penetrate, all microneedles except of two (i.e. 248 of 250), had their membranes broken as a result of the insertion procedure. The two membranes that did not break were located on the same test chip, on needles adjacent to each other and located on the edge of the needle array. Figure 8 shows a SEM picture of a microneedle with

a broken membrane after insertion into human skin. In contrast to the tests on penetrating tissue, tests on fatty tissue, where penetration is less certain, showed different results. Out of the five tests performed, three

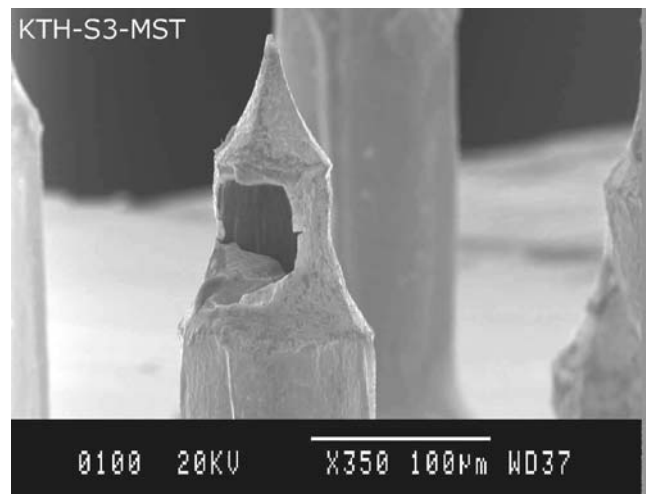


Fig. 8 SEM picture of a circular-shaped microneedle with a broken gold membrane as a result of insertion into living human skin

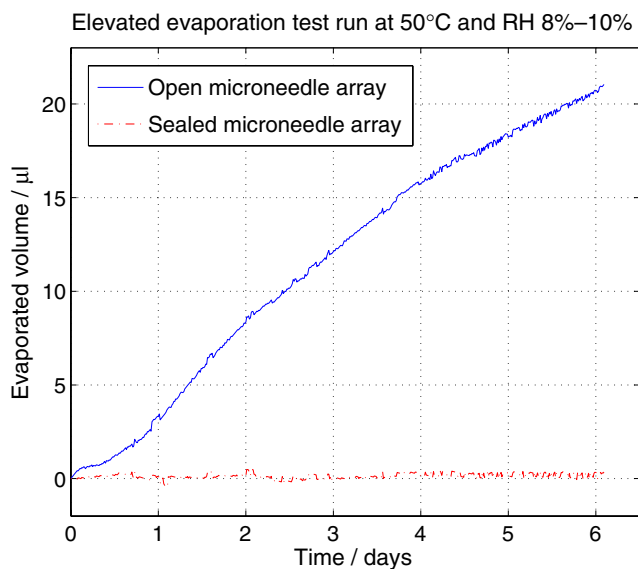


Fig. 9 Evaporation measurement at elevated temperature showing the volatility of DI-water through an unsealed microneedle array (25 microneedles) compared to a 170 nm gold membrane sealed microneedle array. The test is run at 50°C with a relative humidity between 8 and 10%

membranes broke during the insertion procedure (i.e. 3 of 125), two of those were located on the same test chip. Also notable, in some of the trials, membrane residues were observed at the insertion site. Judging from microscope inspection, visible residues seemed to be on the skin surface (in close proximity to the insertion holes). Whether residues also got trapped in the tissue was not possible to determine using the present inspection method. No apparent signs of inflammation (e.g. redness) were observed at the insertion sites, neither directly after the trials nor 24 h later).

Figure 9 shows the result of the elevated evaporation test where a cross-shaped microneedle chip with the thinnest membranes (170 nm) is compared to a non-sealed microneedle chip. No evaporation can be observed from the sealed microneedle chip.

6 Discussion

Taken together, the results from this study show the feasibility of sealed hollow microneedles and possible ways to break the seal at the time of the delivery. The suggested opening schemes may all find their specific advantage for a certain application and drug formulation. For example, a burst type opening scheme may be a useful approach in applications where exact control of the delivered substance is of less importance. Integrated with a simple liquid propulsion mechanism, a patch-like system can be designed where the seals break

once the device is actuated. An example of such an actuator capable of generating pressures above 100 kPa was previously introduced by us (Roxhed et al. 2006), and demonstrated in use with non-sealed microneedles for insulin delivery *in vivo* (Nordquist et al. 2007).

A relatively thick and fairly robust microneedle membrane, that can withstand the forces exerted during the insertion phase into the skin, can be opened electrochemically. Judging from the results, a 170 nm thick gold membrane is too weak to hold during insertion, and thus, considerably thicker seals has to be used which results in longer opening times. Since the removal time for the 170 nm thick membrane was less than 2 min, the time it takes to disrupt a significantly thicker membrane would still only be a matter of minutes. Seen over a total delivery period of hours, this might be an acceptable lag for many formulations. As mentioned earlier, this opening method also adds a possibility for more advanced drug release schemes, e.g. membranes of individual needles may be opened up in a sequential fashion, allowing delivery at specific times.

The burst test measurements show that the membranes can withstand relatively high pressures, well above 100 kPa. Hence, it is reasonable to believe that the membranes can be designed to hold against a static pressure. Utilizing this, an integrated system with a pressurized liquid reservoir can be realized. As shown from the tests on inserting sealed microneedles into skin, a 170 nm thick membrane breaks when the needle is inserted into the tissue. Consequently, a system with a pressurized liquid reservoir and sealed microneedles will start to deliver once the needles penetrate the skin and the membranes break, i.e. such a system would permit active microneedle injection without the need of a power source.

Results from the insertion tests show that microneedle membranes break when inserted into tissue where the needles are known to penetrate. However, the membranes seem to stay intact when the needles are inserted into tissue where penetration is less reliable. This supports the idea that a needle that is not properly inserted into the skin will have its membrane intact and liquid delivery would be blocked. It should be mentioned that the microneedles used in the insertion experiments can also pierce the skin (i.e. breach stratum corneum) at the tested (fatty) insertion site. However, piercing at this site is less reliable and penetration may be limited to the outermost tip, excluding the membrane-covered side-opening. This uncertainty in the degree of penetration may well explain the fact that a few membranes broke also when inserted into fatty tissue.

During fabrication, the gold membranes were deposited on a sacrificial oxide layer which in principle could function as the microneedle seal itself. However, the oxide thickness needed for the fabrication is too thick and thus too strong to be practically useful as a seal. Tests showed that these oxide membranes could withstand a pressure of 600 kPa. By a separate deposition of another membrane layer (e.g. gold), the resulting membranes can be tailored with respect to material properties, thickness and thus mechanical strength.

Of major concern regarding the concept of sealed microneedles is still the biocompatibility. A noble metal seal like gold is, in its natural state, inert to physiological environments and therefore likely to introduce only a weak or no host response. Especially gold has been studied for many years due to its extensive use as a dental material, cf. (Paffenbarger 1972; Walther et al. 2002), but also for other biomedical application, e.g. for coating stents (Edelman et al. 2001). As described earlier, the total mass of the membranes from a microneedle array containing hundreds of needles is a few micrograms. Reported normal value for e.g. gold in human males is less than 10 mg (Venugopal and Luckey 1978). The concentration of gold in the skin under gold finger rings has been reported to 70–90 $\mu\text{g/g}$ skin (Shaw 1991). Microneedle opening methods like burst opening or opening by insertion may leave gold residues both on and in the skin. However, the mass of these residues is relatively low and might therefore be considered as acceptable. In addition, since residues could remain in the dermal tissue, it is worth noting that the skin is constantly renewed with an epidermal turnover time of approximately 30–60 days (Halparin 1972).

In terms of biocompatibility, *in situ* opening by electrochemical etching presents a more questionable method. While gold in its natural inert state is fairly well documented in clinical use, electrochemical etching leads to the formation of chlorogold salts which does not show the same level of documentation. However, in a follow-up study, authors of the previous mentioned implantable drug release chip (Santini et al. 2000) made a rigorous study of the biocompatibility of the gold salts. From trials in a rodent model, they concluded that stimulated gold corrosion *in vivo* was biocompatible (Voskerician et al. 2004).

In summary, the presented concept of sealed hollow microneedles illustrates feasible options to achieve a closed-package transdermal patch in which the drug is released at the time of appliance. In this study, gold membranes were used to seal off side-opened silicon microneedles. However, the presented concept and the

fabrication scheme may be used and adapted to most of the earlier presented microneedle designs.

7 Conclusions

A novel concept of membrane-sealed hollow microneedles for transdermal drug delivery has been introduced. The concept was tested experimentally by sealing side-open silicon microneedles with thin gold membranes. The seals were found leak-tight in an elevated evaporation test and three different opening schemes of the seals were proposed and tested: burst opening, electrochemical opening and opening by insertion into the skin. Tests showed that 170 nm thick gold membranes break when exerted to pressures above 120 kPa. To electrochemically open these membranes in physiological saline, a time of 2 min was required. Membranes of the same thickness were also found to break as a result of microneedle insertion into living skin tissue.

By opening the microneedles seals, there is a risk that membrane residues might remain in the skin tissue once the microneedles has been used and removed. Thus, biocompatibility of the proposed concept is a critical issue. Although biocompatibility was not determined in this study, the fact that possible residues of bioinert gold or gold salts are of minute quantities points towards that the remains could be acceptable.

Altogether, the results of this study show the feasibility of sealed hollow microneedles and how the seals can be opened. This concept is useful in achieving a closed-packaged microneedle-based transdermal patch, which potentially may serve as an alternative to traditional needle injections.

Acknowledgement This work has been funded by the Swedish Foundation for Strategic Research (SSF).

References

- S.P. Davis, B.J. Landis, Z.H. Adams, M.G. Allen, M.R. Prausnitz, J. Biomech. **37**, 1155–1163 (2004)
- E.R. Edelman, P. Seifert, A. Groothuis, A. Morss, D. Bornstein, C. Rogers, Circulation **103**(3), 429–434 (2001)
- N. Fogh-Andersen, B.M. Altura, B.T. Altura, O. Siggaard-Andersen, Clin. Chem. **41**(10), 1522–1525 (1995)
- H.J.G.E. Gardeniers, R. Luttge, E.J.W. Berenschot, M.J. de Boer, S.Y. Yeshurun, M. Hefetz, R. van't Oever, A. van den Berg, IEEE ASME J. Microelectromech. Syst. **12**(6), 855–862 (2003)
- P. Griss and G. Stemme, IEEE ASME J. Microelectromech. Syst. **12**(3), 296–301 (2003)

- K.M. Halparin, Br. J. Dermatol. **86**(1), 14–19 (1972)
- S. Henry, D. McAllister, M.G. Allen, M.R. Prausnitz, J. Pharm. Sci. **87**, 922–925 (1998)
- S. Kaushik, A.H. Hord, D.D. Denson, D.V. McAllister, S. Smitra, M.G. Allen, M.R. Prausnitz, Anesth. Analg. **92**, 502–504 (2001)
- M.M. Levine, Nat. Med. **9**(1), 99–103 (2003)
- W. Lin, M.L. Cormier, A. Samiee, A. Griffin, B. Johnson, C. Teng, G.E. Hardee, P.E. Daddona, Pharm. Res. **18**(12), 1789–1793 (2001)
- W. Martanto, S.P. Davis, H.R. Holiday, J. Wang, H.S. Gill, M.R. Prausnitz, Pharm. Res. **21**(6), 947–952 (2004)
- J.A. Matriano, M. Cormier, J. Johnson, W.A. Young, M. Buttery, K. Nyam, P.E. Daddona, Pharm. Res. **19**(1), 63–70 (2002)
- D.V. McAllister, P.M. Wang, S.P. Davis, J. Park, P.J. Canatella, M.G. Allen, M. Prausnitz, Proc. Natl. Acad. Sci. U. S. A. **100**(24), 13755–13760 (2003)
- J.A. Mikszta, J.B. Alarcon, J.M. Brittingham, D.E. Sutter, R.J. Pettis, N.G. Harvey, Nat. Med. **8**(4), 415–419 (Apr 2002)
- L. Nordquist, N. Roxhed, P. Griss, G. Stemme, Pharm. Res. **24**(7), 1381–1388 (2007)
- G.C. Paffenbarger, J. Am. Dent. Assoc. **84**, 1333–1335 (1972)
- J.-H. Park, M.G. Allen, M.R. Prausnitz, J. Control. Rel. **104**(1), 51–66 (May 2005)
- M.R. Prausnitz, Adv. Drug Deliv. Rev. **56**, 581–587 (2004)
- N. Roxhed, S. Rydholm, B. Samel, W. van der Wijngaart, P. Griss, G. Stemme, J. Micromechanics Microengineering **16**(12), 2740–2746 (2006)
- N. Roxhed, T.C. Gasser, P. Griss, G.A. Holzapfel, G. Stemme, IEEE ASME J. Microelectromech. Syst. (2007a) (in press)
- N. Roxhed, B. Samel, L. Nordquist, P. Griss, G. Stemme, IEEE Trans. Biomed. Eng. (2007b) (in press)
- J.T. Santini, A.C. Richards, R. Scheidt, M.J. Cima, R. Langer, Angew. Chem. Int. Ed. **39**, 2396–2407 (2000)
- C.F. Shaw, *Metals and their compounds in the environment*. (VCH, Weinheim, Germany, 1991), pp. 931–938
- R.K. Sivamani, B. Stoeber, G.C. Wu, H. Zhai, D. Liepmann, H. Maibach, Skin Res. Technol. **11**(11), 152–156 (2005)
- B. Stoeber, D. Liepmann, IEEE ASME J. Microelectromech. Syst. **14**(3), 472–479 (2005), ISSN 1057-7157
- M.A.L. Teo, C. Shearwood, K.C. Ng, J. Lu, S. Mochhala, Biomedical Microdevices **7**(1), 47–52 (2005), ISSN 1387-2176
- B. Venugopal, T.D. Luckey, *Metal toxicity in mammals*, vol. 2. (Plenum Press, New York, 1978), p. 36
- G. Voskerician, R.S. Shawgo, P.A. Hiltner, J.M. Anderson, M.J. Cima, R. Langer, IEEE Trans. Biomed. Eng. **51**(4), 627–635 (2004), ISSN 0018-9294
- U.I. Walther, S.C. Walther, B. Liebl, F.X. Reichl, K. Kehe, M. Nilius, R. Hickel, J. Biomed. Mater. Res. **63**(5), 643–649 (2002)